

Article

Comparative Degradation of a Thiazole Pollutant by an Advanced Oxidation Process and an Enzymatic Approach

Khadega A. Al-Maqdi, Soleiman M. Hisaindee, Muhammad A. Rauf and Syed Salman Ashraf * 

Department of Chemistry, UAE University, P.O. Box 15551, Al-Ain, UAE; 200935138@uaeu.ac.ae (K.A.A.-M.); soleiman.hisaindee@uaeu.ac.ae (S.M.H.); Muhammada@uaeu.ac.ae (M.A.R.)

* Correspondence: salman.ashraf@uaeu.ac.ae; Tel.: +971-03-713-6148; Fax: +971-03-767-1291

Academic Editor: Jürg Bähler

Received: 2 July 2017; Accepted: 22 August 2017; Published: 24 August 2017

Abstract: Organic pollutants, especially those found in water bodies, pose a direct threat to various aquatic organisms as well as humans. A variety of different remediation approaches, including chemical and biological methods, have been developed for the degradation of various organic pollutants. However, comparative mechanistic studies of pollutant degradation by these different systems are almost non-existent. In this study, the degradation of a model thiazole pollutant, thioflavin T (ThT), was carried out in the presence of either an advanced oxidation process (ultraviolet (UV) + H₂O₂) or a chloroperoxidase enzyme system (CPO + H₂O₂). The degradation was followed both spectrophotometrically and using liquid chromatography-mass spectroscopy (LC-MS), and the products formed were identified using tandem liquid chromatography-mass spectrometry-mass spectrometry (LC-MS-MS). The results show that the two remediation approaches produced different sets of intermediates, with only one common species (a demethylated form of ThT). This suggests that different degradation schemes were operating in the two systems. Interestingly, one of the major intermediates produced by the CPO + H₂O₂ system was a chlorinated form of thioflavin. Phytotoxicity studies showed that the CPO + H₂O₂-treated ThT solution was significantly ($p < 0.05$) less toxic than the UV + H₂O₂-treated ThT solution. This is the first time that a comparative mechanistic study showing in detail the intermediates generated in chemical and biological remediation methods has been presented. Furthermore, the results show that different remediation systems have very different degradation schemes and result in products having different toxicities.

Keywords: bioremediation; thiazole; advanced oxidation process; peroxidases; enzymes; chloroperoxidase

1. Introduction

Aromatic compounds are a major class of toxic and potentially carcinogenic organic pollutants that must be removed from effluents before they enter bodies of water [1–3]. Various physical, chemical, and biological approaches have been devised to deal with these contaminants. For example, adsorption, sedimentation, coagulation, membrane filtration, and use of cucurbiturils are all examples of physical processes that have been successfully used to remove various organic pollutants [4,5]. Some of the most commonly used chemical methods include ozonation, NaOCl treatment, and advanced oxidation processes (AOPs) [6,7].

Although physical and chemical methods enjoy wide-scale applicability and are currently used in various large-scale processes, they still face some significant limitations and challenges. The biggest downside of physico-chemical methods are the high costs involved as well as the sludge produced by the processes [4]. Greener alternatives, such as the use of micro-organisms or phytoremediation,

are considered to be more environmentally friendly and have shown promising results for the removal of low concentrations of organic pollutants. Compared with traditional physico-chemical methods, bioremediation may be a safer, less disruptive, and more cost-effective treatment strategy. However, a fundamental shortcoming of bioremediation is that the organisms used for this purpose may be unable to thrive in adverse and unfavorable environmental conditions, as well as the potential inefficiency of the process [8,9].

Enzymatic bioremediation is an emerging method of supplementing bio-treatment techniques. The class of enzyme that is most commonly used for bioremediation purposes is the “oxidoreductase” class of enzymes, which includes oxygenases, monooxygenases, dioxygenases, laccases, and peroxidases. These enzymes carry out redox reactions on a relatively wide range of substrates, including polycyclic aromatic hydrocarbons (PAHs), polynitrated aromatic compounds, pesticides, bleach-plant effluents, synthetic dyes, polymers, and various emerging pollutants [10–13]. Within the oxidoreductase family of enzymes, peroxidases such as lignin peroxidase (LiP), manganese-dependent peroxidase (MnP), versatile peroxidase (VP), soybean peroxidase (SBP), and chloroperoxidase (CPO) have been extensively studied due to their high potential for the degradation of various organic compounds [12,14,15]. It has been postulated that these enzymes could oxidize organic compounds through the generation of reactive free radicals, leading to the formation of lower molecular weight compounds and eventually mineralizing the pollutant. It is worth mentioning that some of the potential shortcomings of using enzymes for large-scale bioremediation purposes are their relatively high costs as well as the lack of the reusability of the enzymes and their stabilities during the remediation processes. However, most of these issues can be ameliorated by employing molecular biology approaches for the microbial recombinant expression of wild-type as well as mutated forms of these enzymes, which can then be immobilized on various supports, such as beads or membranes, to increase their stabilities as well as reusability [16]. The fungus *Caldariomyces fumago* secretes heme-containing CPO, also known as chloride:hydrogen-peroxide oxidoreductase. In addition to catalyzing halogenation reactions, CPO also exhibits peroxidase, catalase, and cytochrome P450-like activities. Although CPO shares common features with other heme-containing enzymes, its structure is unique, being composed of a tertiary assembly consisting primarily of eight helical segments. Our research group and others have used this enzyme for the efficient and rapid degradation of various organic pollutants [17–21]. Although a tremendous amount of research has been published on the use of AOPs [22–24] and enzymatic [18,19,25,26] approaches to the degradation of organic pollutants, including some “combination approaches” [27–31], to date there have been no detailed studies published that compare the degradation of a specific organic compound by these two different methods. Many questions remain about the pollutant degradation pathways, the types of intermediates generated, and the residual toxicity of the pollutants when using these two very different methods. The ultraviolet (UV) + H₂O₂ AOP approach relies on the pollutant molecules reacting with the hydroxyl radicals generated upon the photolysis of H₂O₂, whereas the CPO enzyme method relies on the enzyme heme-iron oxyl radical. Therefore, it is expected that there may be significant differences in the intermediates produced during the two processes.

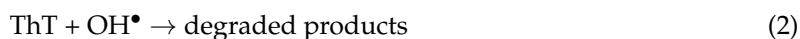
The aim of present study was to compare the degradation of a thiazole compound (thioflavin T, ThT) when using the classical UV + H₂O₂ AOP method and the CPO + H₂O₂ based approach. ThT can prove to be a useful model for pollution remediation studies, as its thiazole core is a common feature in some of the important emerging pollutants, such as 2-mercaptobenzothiazole (a plasticizer/vulcanizing agent), Thiabendazole and Tricyclazole (fungicidal drugs), and Meloxicam, (a non-steroidal anti-inflammatory drug). Alarmingly, all of these and other thiazole derivatives have been detected in various aquatic environments [32,33]. Moreover, as ThT is a colored compound, colorimetric changes during degradation can be monitored easily and efficiently using spectrophotometry. This study also carried out an liquid chromatography-mass spectrometry-mass spectrometry (LC-MS-MS)-based investigation to allow for a comparison of the mechanistic

degradation pathways of the two remediation methods. Finally, phytotoxicity analyses were carried out to measure the residual toxicity of ThT after treatment with the AOP and CPO-based systems.

2. Results and Discussion

2.1. Degradation of ThT by UV + H₂O₂

In the present work, we initially investigated the H₂O₂-assisted photochemical oxidation of ThT. Figure 1 shows the chemical structure as well as the absorption spectrum of ThT. Also shown is the major peak in the yellow visible region of the ThT absorption spectrum ($\lambda_{\max} = 412$ nm). The exposure of the ThT solution to UV + H₂O₂ caused an immediate and gradual decrease in the intensity of λ_{\max} , indicating that new compounds had formed. Figure 1B shows the degradation of λ_{\max} as a function of time, and it can be seen that about 70% of the compound had degraded after 60 min of this AOP treatment. No ThT degradation was observed in the presence of UV light or H₂O₂ alone. The degradation of ThT was attributed to the hydroxyl radicals (OH•) produced from H₂O₂ when exposed to UV radiation. Hydroxyl radicals are known to be strong oxidizing agents that can react with ThT molecules to produce intermediates that are responsible for decoloring/degradation of the original solution [34,35]. A simplified reaction scheme for this process is outlined below:



The results obtained here are consistent with numerous studies by our group and others, which show that UV + H₂O₂ can readily degrade an array of organic compounds [36,37].

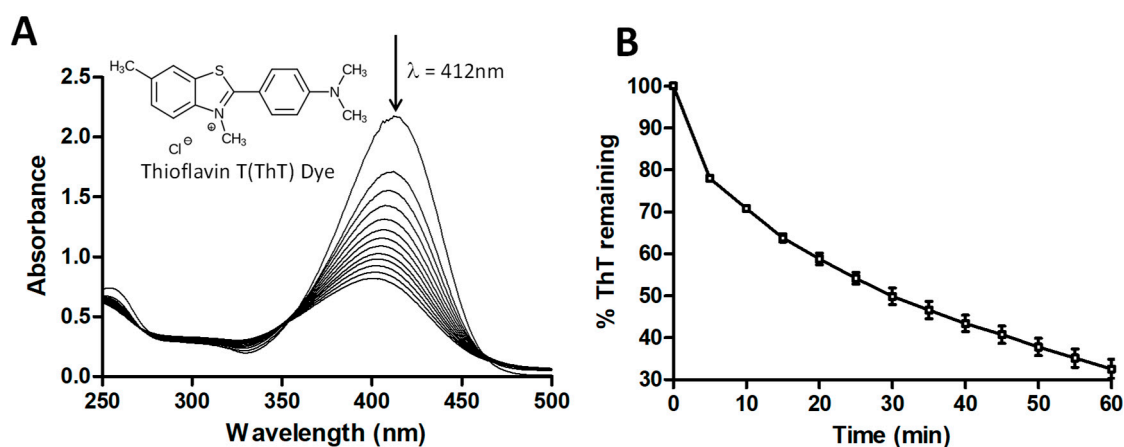


Figure 1. Thioflavin T (ThT) dye degradation by a UV + H₂O₂ advanced oxidation process. (A) ultraviolet/visible (UV/Vis) absorbance spectra for ThT degradation by UV + H₂O₂. Concentration of ThT dye = 25 ppm, pH = 2, concentration of H₂O₂ = 1 mM. The UV/Vis scans were taken every 5 min; (B) Percentage of ThT remaining (decrease in absorbance at 412 nm) after treatment with UV + H₂O₂. Concentration of ThT dye = 25 ppm, pH = 2, concentration of H₂O₂ = 1 mM. Data shown is the average of triplicate measurements (\pm standard deviation (SD)).

2.2. Degradation of ThT by CPO + H₂O₂

In order to compare the UV + H₂O₂-induced degradation of ThT with an enzymatic approach, we used the well-known peroxidase CPO to degrade ThT.

Figure 2 shows the absorbance spectra of ThT when exposed to CPO + H₂O₂ as a function of time. As was seen for the UV + H₂O₂ degradation of ThT in Figure 1, the ThT started to degrade immediately upon exposure to CPO + H₂O₂, as evidenced by the decrease in the absorbance at 412 nm. Interestingly, as the peak at 412 nm decreased in intensity, a new peak with $\lambda_{\max} = 350$ nm appeared, with the

intensity of this peak increasing over time. This is shown more clearly in Figure 2B. The increase in the absorbance this peak suggests that a new compound was being generated upon the treatment of ThT with CPO + H₂O₂, something that was not seen in the case of the UV + H₂O₂ treatment of ThT. This observation suggests that the UV + H₂O₂ and CPO + H₂O₂ processes likely have different effects on ThT.

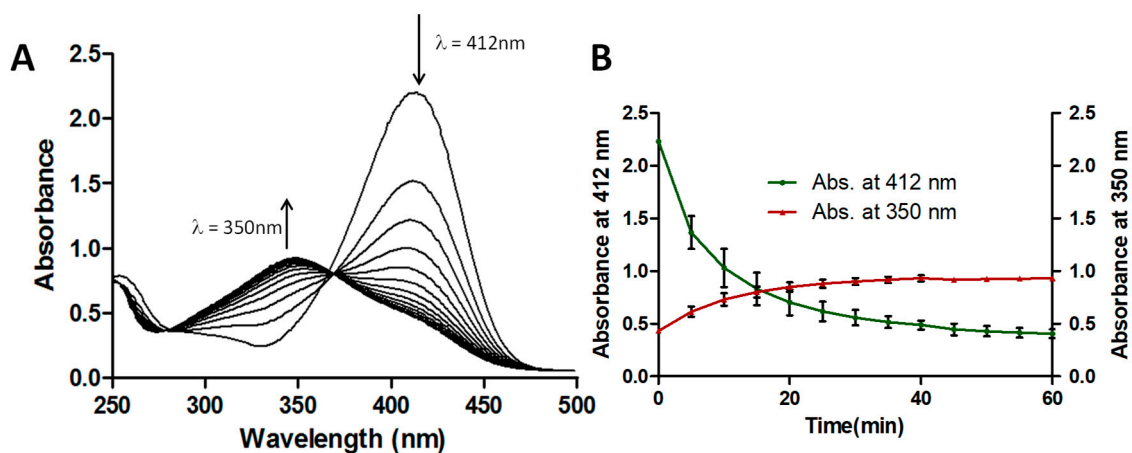


Figure 2. ThT dye degradation by Chloroperoxidase (CPO) + H₂O₂. (A) UV/Vis absorbance spectra for ThT dye degradation by CPO + H₂O₂. Concentration of ThT dye = 25 ppm, pH = 2, concentration of H₂O₂ = 1 mM, concentration of CPO = 10 nM. The UV/Vis scans were taken every 5 min; (B) Changes in absorbances at 412 nm and 350 nm of ThT dye after treatment with CPO + H₂O₂. Concentration of ThT dye = 25 ppm, pH = 2, concentration of H₂O₂ = 1 mM, concentration of CPO = 10 nM. Data shown is the average of triplicate measurements (\pm SD).

2.3. Analysis of Product Formation Using LC-MS

Since the UV/Vis spectroscopic data for degradation of ThT by UV + H₂O₂ and CPO + H₂O₂ suggested that different degradative pathways might be operating in the two remediation methods, we wanted to confirm this using liquid chromatography-mass spectroscopy (LC-MS). Figure 3 shows the LC-MS chromatograms of ThT, ThT exposed to UV + H₂O₂, and ThT treated with CPO + H₂O₂. Additionally, the insets show the mass spectra of the major peaks in the three samples. The LC-MS analysis of the neat ThT dye shows a single major peak at a retention time of 16.11 min, with $m/z = 283$ (inset). This molecular weight (MW) is in agreement with the loss of the chloride counter ion from the molecular weight of the ThT dye (MW = 318.86 Da), which would be expected as the LC-MS system was operating in the positive mode. The LC-MS analysis of the ThT + UV + H₂O₂ sample shows a much smaller ThT peak (retention time = 16.11 min), which is consistent with the degradation of ThT. However, another major peak can also be seen at a retention time of 15.64 min. The mass spectrum of this new product peak (inset) shows it to have an m/z value of 269. In addition to this major product peak, several other smaller peaks can also be seen at the 14–16 min range. The LC-MS analysis of the ThT dye treated with CPO + H₂O₂ shows a very different LC profile, with the major peak having a retention time of 16.19 min. The mass spectrum of this peak shows it to have an m/z value of 317, indicating the presence of a compound that is very different from both the original ThT ($m/z = 283$) and the major intermediate produced during the UV/H₂O₂ AOP degradation of ThT ($m/z = 269$). In addition to this $m/z = 317$ peak, additional minor peaks can also be seen in the ThT + CPO + H₂O₂ sample.

Detailed analyses of all the peaks detected after the UV + H₂O₂ and CPO + H₂O₂ treatments of ThT are shown in Table 1. As can be seen from this table, the AOP-mediated degradation of ThT (ThT + UV + H₂O₂) generated four intermediates with m/z values of 297, 288, 269, and 255, with the $m/z = 269$ peak being the most prominent intermediate (based on peak area). Interestingly, the intermediates produced during the enzymatic treatment of ThT (ThT + CPO + H₂O₂) were

very different, with m/z values of 397, 361, 351, 321, 317, 303, 289, and 269. It is worth noticing that except for the $m/z = 269$ species, the two different treatments produced completely different intermediates. This interesting and novel finding is also graphically represented in Figure 4.

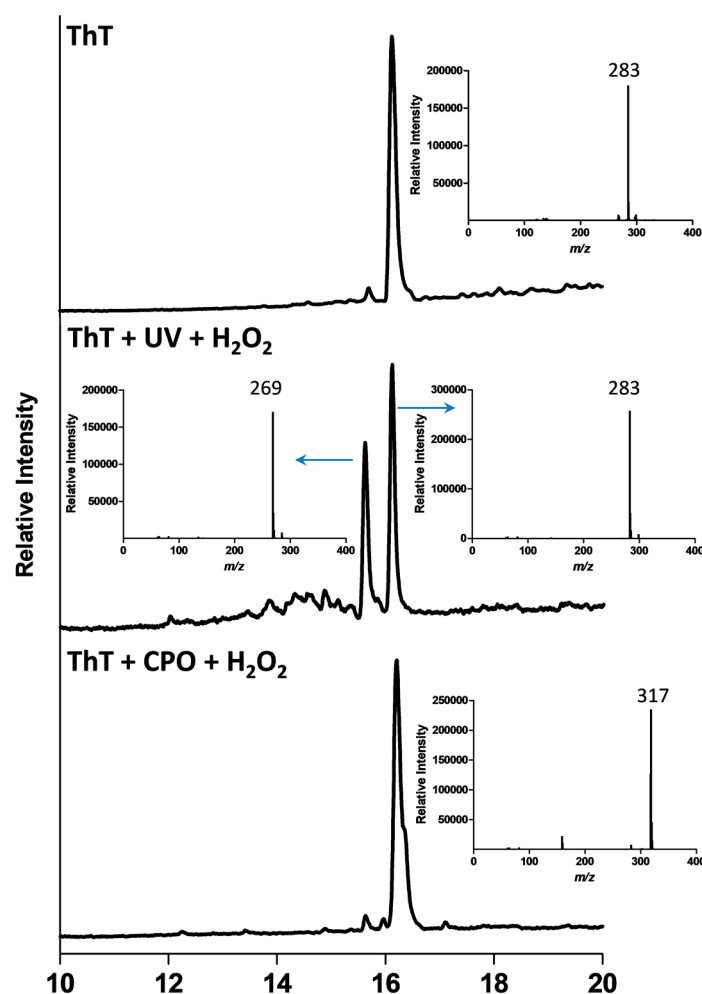


Figure 3. Liquid chromatography-mass spectrometry (LC-MS) chromatogram and mass spectrometry-mass spectrometry (MS-MS) analyses of ThT degraded by UV + H₂O₂ and CPO + H₂O₂ processes. The conditions for UV + H₂O₂ degradation were: concentration of ThT = 25 ppm, pH = 2, concentration of H₂O₂ = 1 mM, and for CPO + H₂O₂ degradation: concentration of ThT dye = 25 ppm, pH = 2, concentration of H₂O₂ = 1 mM, concentration of CPO = 10 nM.

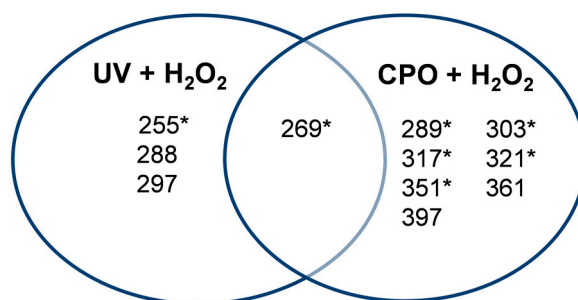


Figure 4. Summary of the intermediates produced upon ThT degradation by UV + H₂O₂ and CPO + H₂O₂ processes. The asterisk (*) indicate intermediates whose structures are shown in Figure 6A,B.

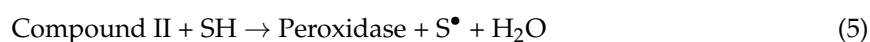
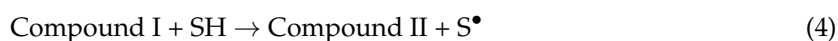
Table 1. Peak area of intermediates produced during the degradation of ThT by UV + H₂O₂ and CPO + H₂O₂ processes.

Retention Time (min)	ThT + UV + H ₂ O ₂		ThT + CPO + H ₂ O ₂	
	<i>m/z</i>	Peak Area	<i>m/z</i>	Peak Area
14.35	288	24,398	-	-
14.86	255	161,335	-	-
15.11	297	70,562	-	-
15.39	-	-	289	27,169
15.64	269	1,216,238	269	300,854
15.97	-	-	303	190,007
16.11	283	1,789,254	283	249,499
16.19	-	-	317	6,147,872
16.21	-	-	321	138,735
16.38	-	-	361	639,968
17.11	-	-	351	81,812
17.27	-	-	397	9,472

2.4. Mechanistic Studies

An attempt was made to propose plausible structures for the various different intermediates generated in the two different treatments by using tandem mass spectrometry-mass spectrometry (MS-MS) data. Indeed, as can be seen in Figure 5, we were able to propose structures for seven of the intermediates produced, with the relevant peaks being indicated by asterisks (*) in Figure 4. Based on the structure of the intermediates, we were able to develop plausible schemes for ThT breakdown during the UV + H₂O₂ and CPO + H₂O₂ remediation processes. In the UV + H₂O₂ process, the main mechanism involves the formation of OH• radicals by the UV-mediated homolysis of hydrogen peroxide. These reactive OH• radicals attack ThT, leading to the stepwise demethylation of the tertiary amine and resulting in the formation of intermediates with *m/z* values of 269. Subsequent demethylation produces the *m/z* = 255 compound. This demethylation mechanism has been previously reported by our group as well as others [38–40]. The decrease in the retention times of these intermediates (15.64 min and 15.8 min) on the reverse-phase column when compared to ThT (16.11 min) reflects their increased polarities. Other, more polar intermediates with *m/z* values of 297 and 288 and retention times of 15.11 and 14.35 min, respectively, were also produced during the UV + H₂O₂ treatment of ThT.

Unlike the UV-induced photolysis of H₂O₂, which generates reactive hydroxyl radicals, the CPO + H₂O₂ system entails a different mechanism. It is well-known that heme peroxidases, such as CPO, can react with H₂O₂ to generate an enzymatic iron oxyradical called Compound I, which can react with organic substrates to be converted to the Compound II form of the enzyme and an organic radical. The Compound II form of the enzyme can react with another organic substrate to create another organic radical molecule and regenerate the resting form of the enzyme [9], as shown below:



where SH indicates a generic substrate.

Although the above peroxidase reaction cycle does not explicitly show the generation of hydroxyl radicals, it is possible that OH radicals may also be produced in this case, as CPO is known to cleave the peroxide O–O bond through a glutamic acid residue present in its active site [41].

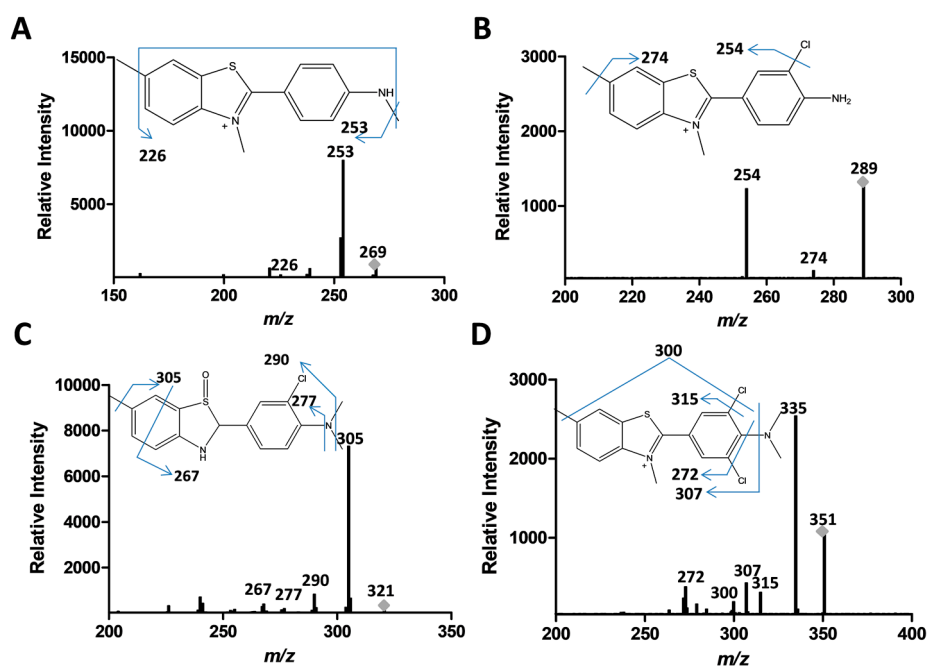
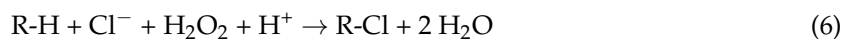


Figure 5. Tandem mass spectrometry fragmentation analyses of proposed intermediates produced after ThT degradation by UV + H₂O₂ (*m/z* of 269, panel (A)) or CPO + H₂O₂ as shown in panels (A,B) (*m/z* of 289); (C) (*m/z* of 321) and (D) (*m/z* of 351).

Besides the well-known H₂O₂-peroxidase cycle described above, CPO is also known to catalyze chlorination of organic compounds [18,42], as shown below:



In fact, based on the MS-MS data, our proposed degradation scheme suggests that the action of CPO on ThT in the presence of H₂O₂ can occur through two overlapping pathways, with the first being the chlorination of ThT, and the second being the production of OH• that can react with ThT and its chlorinated products (Figure 6B). A comparison of the abundance of the proposed species (Table 1) as determined by LC-MS-MS suggests that the chlorination pathway (317 *m/z* species) was at least twenty times more active than the demethylation pathway (269 *m/z* species). A second chlorination also occurs, yielding a compound with an *m/z* value of 351 (Figure 5D). The mono-chlorinated ThT could also undergo stepwise demethylation, yielding structures with *m/z* values of 303 and 289. An intermediate with *m/z* = 321 was also observed, which corresponds to the addition of an OH (oxidation) to the demethylated form of chlorinated ThT, as seen in Figure 6B.

The generation of chlorinated products of ThT observed during the CPO + H₂O₂ treatment of ThT was not completely unexpected, as ThT contains a chloride counter ion and it is well-established that CPO, in the presence of halide ions can lead to the halogenation of various organic substrates [43]. In fact, we have previously published that in contrast to ThT, a different but related thiazole compound (2-mercaptobenzothiazole), which did not contain a chloride counterion, did not produce any chlorinated products [18]. However, it is expected that most industrial waste streams would have relatively high concentrations of various ions, including halides [44], and hence the results presented here could be valuable and relevant in real life remediation situations.

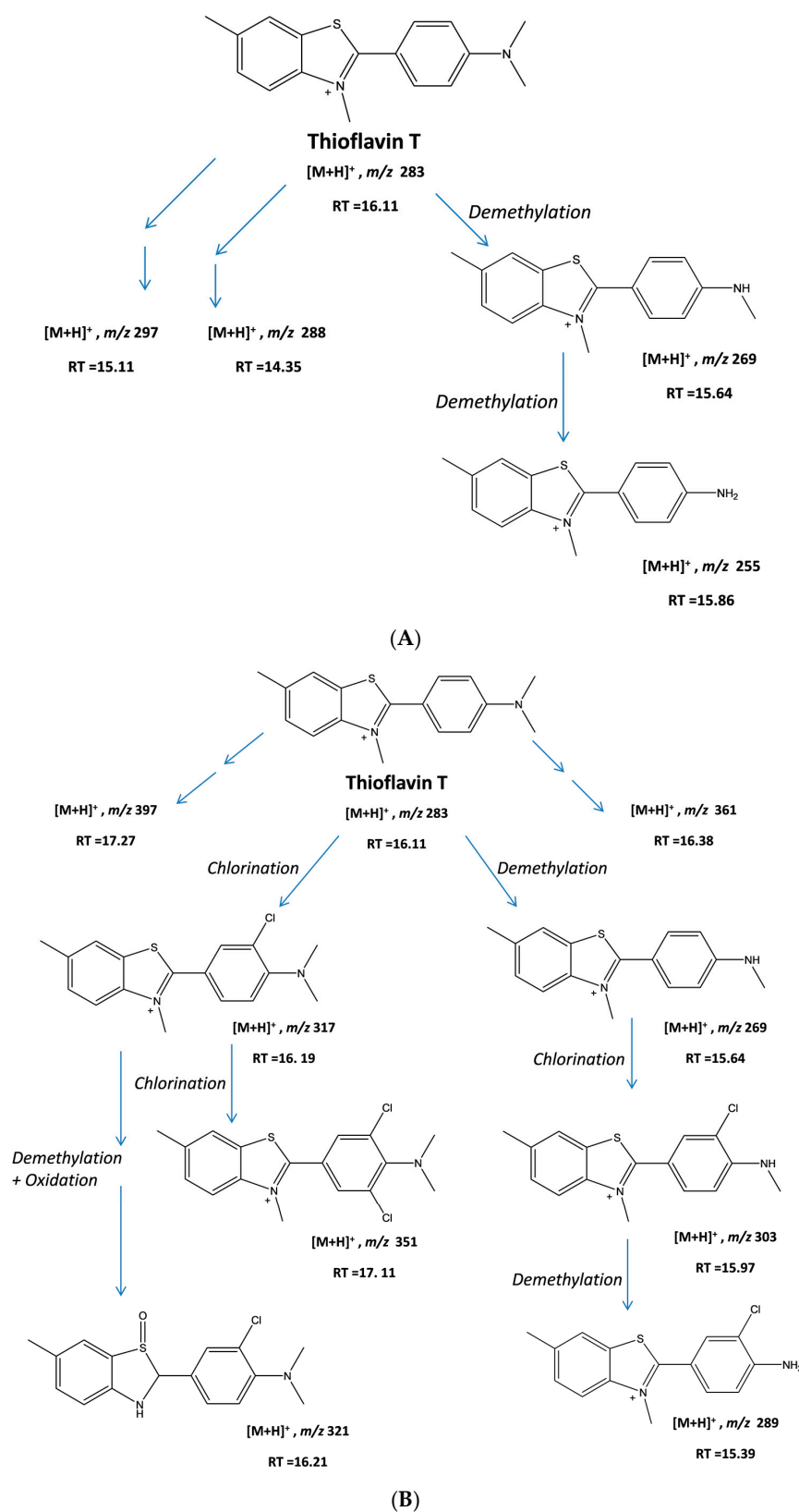


Figure 6. (A) Proposed structures of some of the intermediates generated during the UV + H₂O₂-based degradation of ThT dye; (B) Proposed structures of some of the intermediates generated during the CPO + H₂O₂-based degradation of ThT dye. RT: retention time.

2.5. Toxicity Studies

The toxicity of degradation products should be analyzed where possible, as they can often be more toxic than the parent compound [45]. Therefore, we carried out phytotoxicity studies using *Lactuca sativa* seeds by exposing them to AOP-remediated ThT and enzymatically treated ThT solutions. The germination of *Lactuca sativa* L. var. *Buttercrunch* seeds is a standard protocol for assessing toxicity in water and soil matrices, and is recommended for bioassays by the U.S. Environmental Protection Agency, the Food and Drug Administration, and the Organization for Economic Cooperation and Development [46]. Figure 7 shows the results of the toxicity studies, in which the root lengths of *L. sativa* seeds exposed to distilled water (control), neat ThT, ThT treated with UV + H₂O₂, or ThT treated with CPO + H₂O₂ were measured. As can be seen from the figure, ThT had a significant phytotoxic effect on the seeds, causing a dramatic and significant decrease in the mean root length. A significant inhibition of root lengths was also observed in the ThT + UV + H₂O₂ and ThT + CPO + H₂O₂ samples (Figure 7). However, a *t*-test analysis showed that the ThT + CPO + H₂O₂ sample was significantly ($p < 0.05$) less toxic than the ThT + UV + H₂O₂ sample. This result was quite unexpected, and suggests that one or more of the intermediates generated during the UV + H₂O₂ treatment of ThT could be toxic. Alternatively, the fact that the ThT + CPO + H₂O₂ sample still exhibited significant phytotoxicity could be explained by the fact that this sample still contained large amounts of the toxic undegraded ThT dye. Further studies will need to be carried out to allow the nature of the phytotoxicity of the ThT + UV + H₂O₂ sample to be understood; however, the present data shows that the UV + H₂O₂ and CPO + H₂O₂ treatments of ThT produce different intermediates that could have differing toxicities: an observation that has not been published earlier.

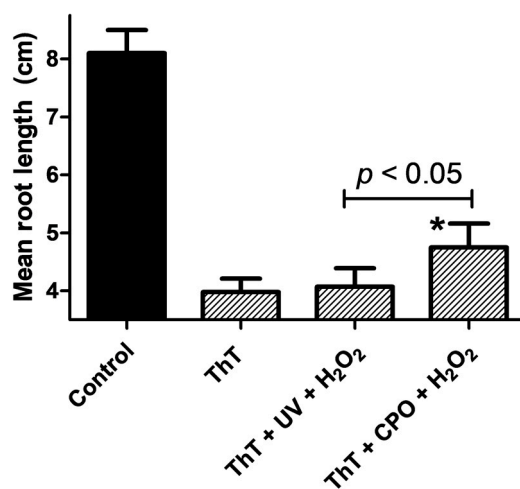


Figure 7. ThT dye toxicity on *Lactuca sativa* seeds, as measured by the mean root lengths (cm) of seeds after treatment with ThT dye (25 ppm), ThT dye treated by UV + H₂O₂, or ThT dye treated by CPO + H₂O₂. Statistical analyses were performed using an unpaired *t*-test ($n = 40$); asterisk (*) denotes a significant difference ($p < 0.05$).

3. Materials and Methods

3.1. Reagents

The thiazole compound thioflavin T (whose molecular formula is C₁₇H₁₉ClN₂S and whose formula weight is 318.86 g·mol⁻¹) was purchased from AnaSpec (Fremont, CA, USA). Hydrogen peroxide (30% *w/v*) and LC-MS grade solvents, such as formic acid and acetonitrile, were purchased from Sigma-Aldrich (St. Louis, MO, USA). All of the experiments were carried out in 50 mM citrate buffer, pH 2. CPO with a specific activity of 1296 IU/mg (17 mg/mL, 405 μM) was purchased from Bio-Research Products (North Liberty, IA, USA).

3.2. Thioflavin T Decolorization

For the photolytic treatment of ThT using UV + H₂O₂, 1 mM H₂O₂ was added to ThT samples in 50 mM citrate buffer (pH 2), which were then irradiated with a UV lamp (UVGL-58, J-129, Upland, NJ, USA) from a distance of 1.5 cm. The instrument had a UV power output of 6 W and was selectively used in the 254 nm output mode for these studies. Under these conditions, no significant warming up of the irradiated solution was observed.

For the enzymatic treatment of ThT using CPO + H₂O₂, experiments were carried out as previously described [18]. Briefly, ThT and H₂O₂ (1 mM) in 50 mM citrate buffer (pH 2) was exposed to CPO (10 nM), and the changes in the full ThT spectrum were monitored.

In both the enzymatic and the photolytic studies, spectra were collected in the range of 200–800 nm using a Carry 60 Spectrophotometer (Agilent Technologies, Santa Clara, CA, USA), with a path length of 1 cm (4 mL quartz cuvette) and 412 nm was used as λ_{max} .

3.3. LC-MS and MS-MS Analyses

The materials produced after the enzymatic and the photolytic treatments were analyzed using LC-MS, as previously described [18,19]. Briefly, all ThT samples were filtered using a 0.45 μm CA syringe filter prior to injection. The LC-MS was fitted with a ZORBAX Eclipse Plus C18 column (Agilent Technologies, Santa Clara, CA, USA) with a particle size of 1.8 μm , an inner diameter of 2.1 mm, and a length of 50 mm. The column was maintained at 35 °C, and a constant flow rate of 0.2 mL/min was maintained. The column was coupled to a 6420 Triple Quad LC-MS System detector (Agilent Technologies). Two mobile phases were used: A is water containing 0.1% formic acid, and B is 100% acetonitrile. The LC method was set as follows: 5 min of 100% A, followed by a 0–100% gradient of B from 5–20 min, then 5 min of 100% B after the gradient, and finally 5 min of 100% A. The electrospray ionization source in the LC-MS system was in positive polarity mode, the capillary voltage was set at 4000 V, the nebulizer pressure was maintained at 45 psi, the drying gas (N₂) flow was 11 L/min, and the drying temperature was set at 325 °C. The mass range monitored for all of the runs was between 50 and 1000 Da. In the tandem MS experiments using the product ion mode, nitrogen gas was used for fragmentation and different collision energies were used.

3.4. Phytotoxicity Assay

The toxicity of ThT before and after the UV + H₂O₂ and CPO + H₂O₂ treatments was measured using the lettuce seed growth inhibition assay, similar to a previously described method but with slight modifications [19]. Briefly, 20 *Lactuca sativa* seeds were placed on sterilized Whatman filter paper, No. 3, in a Petri dish and saturated with 4 mL of the samples. The petri dishes were incubated for 5 days in a humidified chamber at 25 \pm 2 °C. Distilled water was used as a negative control and ThT was used as a positive control, with each sample being tested in duplicate. The effects of the original dye and the dye samples degraded by UV + H₂O₂ and CPO + H₂O₂ were examined by measuring the lengths of the roots of the germinated seeds. Statistical analyses were conducted for each group of treated seeds ($n = 40$). The data were analyzed via unpaired *t*-tests. Data are reported as group mean \pm standard deviation, and significance for all statistical comparisons was set at $p < 0.05$.

4. Conclusions

To the best of our knowledge, this is the first study to present a systematic comparison of the use of two different remediation methods to treat a toxic organic pollutant. We showed that treating ThT with UV + H₂O₂ and CPO + H₂O₂ produced very different degradation products, with only one common intermediate. This suggested that different organic pollutant degradation schemes were involved in these two remediation approaches, and we attempted to elucidate these mechanisms. Additionally, we showed that the AOP (UV + H₂O₂) and enzymatic (CPO + H₂O₂) treated ThT solutions had significantly different toxicities for *L. sativa* seeds. The unexpected and intriguing data presented

here also highlights the need for a better understanding of different remediation approaches and for additional research into such comparative remediation studies.

Acknowledgments: The authors acknowledge the generous funding from the United Arab Emirates University National Water Center, grant ID 31R078, to Syed Salman Ashraf.

Author Contributions: Syed Salman Ashraf conceived and designed the experiments; Khadega A. Al-Maqdi performed the experiments; Khadega A. Al-Maqdi, Soleiman M. Hisaindee and Syed Salman Ashraf analyzed the data; all authors contributed to the writing of the manuscript.

Conflicts of Interest: The authors declare no conflict of interest.

References

1. Ebele, A.J.; Abou-Elwafa Abdallah, M.; Harrad, S. Pharmaceuticals and personal care products (PPCPs) in the freshwater aquatic environment. *Emerg. Contam.* **2017**, *3*, 1–16. [[CrossRef](#)]
2. Stuart, M.; Lapworth, D.; Crane, E.; Hart, A. Review of risk from potential emerging contaminants in UK groundwater. *Sci. Total Environ.* **2012**, *416*, 1–21. [[CrossRef](#)] [[PubMed](#)]
3. Lapworth, D.J.; Baran, N.; Stuart, M.E.; Ward, R.S. Emerging organic contaminants in groundwater: A review of sources, fate and occurrence. *Environ. Pollut.* **2012**, *163*, 287–303. [[CrossRef](#)] [[PubMed](#)]
4. Robinson, T.; McMullan, G.; Marchant, R.; Nigam, P. Remediation of dyes in textile effluent: A critical review on current treatment technologies with a proposed alternative. *Bioresour. Technol.* **2001**, *77*, 247–255. [[CrossRef](#)]
5. Adeleye, A.S.; Conway, J.R.; Garner, K.; Huang, Y.; Su, Y.; Keller, A.A. Engineered nanomaterials for water treatment and remediation: Costs, benefits, and applicability. *Chem. Eng. J.* **2016**, *286*. [[CrossRef](#)]
6. Bokare, A.D.; Choi, W. Review of iron-free Fenton-like systems for activating H₂O₂ in advanced oxidation processes. *J. Hazard. Mater.* **2014**, *275*, 121–135. [[CrossRef](#)] [[PubMed](#)]
7. Kalsoom, U.; Ashraf, S.S.; Meetani, M.A.; Rauf, M.A.; Bhatti, H.N. Degradation and kinetics of H₂O₂ assisted photochemical oxidation of Remazol Turquoise Blue. *Chem. Eng. J.* **2012**, *200*, 373–379. [[CrossRef](#)]
8. Boopathy, R. Factors limiting bioremediation technologies. *Bioresour. Technol.* **2000**, *74*, 63–67. [[CrossRef](#)]
9. Rauf, M.A.; Salman Ashraf, S. Survey of recent trends in biochemically assisted degradation of dyes. *Chem. Eng. J.* **2012**, *209*, 520–530. [[CrossRef](#)]
10. Ali, L.; Algaithi, R.; Habib, H.M.; Souka, U.; Rauf, M.A.; Ashraf, S.S. Soybean peroxidase-mediated degradation of an azo dye—a detailed mechanistic study. *BMC Biochem.* **2013**, *14*, 35. [[CrossRef](#)] [[PubMed](#)]
11. Bibi, I.; Bhatti, H.N.; Asgher, M. Comparative study of natural and synthetic phenolic compounds as efficient laccase mediators for the transformation of cationic dye. *Biochem. Eng. J.* **2011**, *56*, 225–231. [[CrossRef](#)]
12. Kalsoom, U.; Ashraf, S.S.; Meetani, M.A.; Rauf, M.A.; Bhatti, H.N. Mechanistic study of a diazo dye degradation by Soybean Peroxidase. *Chem. Cent. J.* **2013**, *7*, 93. [[CrossRef](#)] [[PubMed](#)]
13. Franciscan, E.; Piubeli, F.; Fantinatti-Garboggini, F.; Ragagnin de Menezes, C.; Serrano Silva, I.; Cavaco-Paulo, A.; Grossman, M.J.; Durrant, L.R. Polymerization study of the aromatic amines generated by the biodegradation of azo dyes using the laccase enzyme. *Enzym. Microb. Technol.* **2010**, *46*, 360–365. [[CrossRef](#)]
14. Ryan, B.J.; Carolan, N.; ÓFágáin, C. Horseradish and soybean peroxidases: Comparable tools for alternative niches? *Trends Biotechnol.* **2006**, *24*, 355–363. [[CrossRef](#)] [[PubMed](#)]
15. Cheng, X.-B.; Jia, R.; Li, P.-S.; Zhu, Q.; Tu, S.-Q.; Tang, W.-Z. Studies on the Properties and Co-immobilization of Manganese Peroxidase. *Chin. J. Biotechnol.* **2007**, *23*, 90–96. [[CrossRef](#)]
16. Adrio, J.L.; Demain, A.L. Microbial Enzymes: Tools for Biotechnological Processes. *Biomolecules* **2014**, *4*, 117–139. [[CrossRef](#)] [[PubMed](#)]
17. Liu, L.; Zhang, J.; Tan, Y.; Jiang, Y.; Hu, M.; Li, S.; Zhai, Q. Rapid decolorization of anthraquinone and triphenylmethane dye using chloroperoxidase: Catalytic mechanism, analysis of products and degradation route. *Chem. Eng. J.* **2014**, *244*, 9–18. [[CrossRef](#)]
18. Alneyadi, A.H.; Ashraf, S.S. Differential enzymatic degradation of thiazole pollutants by two different peroxidases—A comparative study. *Chem. Eng. J.* **2016**, *303*, 529–538. [[CrossRef](#)]
19. Alneyadi, A.H.; Shah, I.; AbuQamar, S.F.; Ashraf, S.S. Differential Degradation and Detoxification of an Aromatic Pollutant by Two Different Peroxidases. *Biomolecules* **2017**, *7*, 31. [[CrossRef](#)] [[PubMed](#)]

20. Sundaramoorthy, M.; Ternner, J.; Poulos, T.L. The crystal structure of chloroperoxidase: A heme peroxidase—cytochrome P450 functional hybrid. *Structure* **1995**, *3*, 1367–1378. [[CrossRef](#)]
21. Hofrichter, M.; Ullrich, R.; Pecyna, M.J.; Liers, C.; Lundell, T. New and classic families of secreted fungal heme peroxidases. *Appl. Microbiol. Biotechnol. Heidelb.* **2010**, *87*, 871–897. [[CrossRef](#)] [[PubMed](#)]
22. Abdelraheem, W.H.M.; He, X.; Komy, Z.R.; Ismail, N.M.; Dionysiou, D.D. Revealing the mechanism, pathways and kinetics of UV_{254nm}/H₂O₂-based degradation of model active sunscreen ingredient PBSA. *Chem. Eng. J.* **2016**, *288*, 824–833. [[CrossRef](#)]
23. Oturan, M.A.; Aaron, J.-J. Advanced Oxidation Processes in Water/Wastewater Treatment: Principles and Applications. A Review. *Crit. Rev. Environ. Sci. Technol.* **2014**, *44*, 2577–2641. [[CrossRef](#)]
24. Cesaro, A.; Belgiorno, V. Removal of Endocrine Disruptors from Urban Wastewater by Advanced Oxidation Processes (AOPs): A Review. *Open Biotechnol. J.* **2016**, *10*. [[CrossRef](#)]
25. Rodríguez-Delgado, M.; Ornelas-Soto, N. Laccases: A Blue Enzyme for Greener Alternative Technologies in the Detection and Treatment of Emerging Pollutants. In *Green Technologies and Environmental Sustainability*; Springer: Cham, Switzerland, 2017; pp. 45–65, ISBN 978-3-319-50653-1.
26. Dhillon, G.S.; Kaur, S. *Agro-Industrial Wastes as Feedstock for Enzyme Production: Apply and Exploit the Emerging and Valuable Use Options of Waste Biomass*; Academic Press: Cambridge, MA, USA, 2016, ISBN 978-0-12-802612-0.
27. Calza, P.; Avetta, P.; Rubulotta, G.; Sangermano, M.; Laurenti, E. TiO₂-soybean peroxidase composite materials as a new photocatalytic system. *Chem. Eng. J.* **2014**, *239*, 87–92. [[CrossRef](#)]
28. Nogueira, V.; Lopes, I.; Freitas, A.C.; Rocha-Santos, T.A.P.; Gonçalves, F.; Duarte, A.C.; Pereira, R. Biological treatment with fungi of olive mill wastewater pre-treated by photocatalytic oxidation with nanomaterials. *Ecotoxicol. Environ. Saf.* **2015**, *115*, 234–242. [[CrossRef](#)] [[PubMed](#)]
29. García-Montaño, J.; Domènech, X.; García-Hortal, J.A.; Torrades, F.; Peral, J. The testing of several biological and chemical coupled treatments for Cibacron Red FN-R azo dye removal. *J. Hazard. Mater.* **2008**, *154*, 484–490. [[CrossRef](#)] [[PubMed](#)]
30. García-Montaño, J.; Pérez-Estrada, L.; Oller, I.; Maldonado, M.I.; Torrades, F.; Peral, J. Pilot plant scale reactive dyes degradation by solar photo-Fenton and biological processes. *J. Photochem. Photobiol. Chem.* **2008**, *195*, 205–214. [[CrossRef](#)]
31. Sánchez Pérez, J.A.; Carra, I.; Sirtori, C.; Agüera, A.; Esteban, B. Fate of thiabendazole through the treatment of a simulated agro-food industrial effluent by combined MBR/Fenton processes at µg/L scale. *Water Res.* **2014**, *51*, 55–63. [[CrossRef](#)] [[PubMed](#)]
32. Clarke, B.O.; Smith, S.R. Review of “emerging” organic contaminants in biosolids and assessment of international research priorities for the agricultural use of biosolids. *Environ. Int.* **2011**, *37*, 226–247. [[CrossRef](#)] [[PubMed](#)]
33. Collado, N.; Rodríguez-Mozaz, S.; Gros, M.; Rubirola, A. Pharmaceuticals occurrence in a WWTP with significant industrial contribution and its input into the river system. *Environ. Pollut.* **2014**, *185*, 202–212. [[CrossRef](#)] [[PubMed](#)]
34. Konstantinou, I.K.; Albanis, T.A. TiO₂-assisted photocatalytic degradation of azo dyes in aqueous solution: Kinetic and mechanistic investigations. *Appl. Catal. B Environ.* **2004**, *49*, 1–14. [[CrossRef](#)]
35. Georgiou, D.; Melidis, P.; Aivasidis, A.; Gimouhopoulos, K. Degradation of azo-reactive dyes by ultraviolet radiation in the presence of hydrogen peroxide. *Dyes Pigments* **2002**, *52*, 69–78. [[CrossRef](#)]
36. Rauf, M.A.; Ali, L.; Sadig, M.S.A.Y.; Ashraf, S.S.; Hisaindee, S. Comparative degradation studies of Malachite Green and Thiazole Yellow G and their binary mixture using UV/H₂O₂. *Desalination Water Treat.* **2016**, *57*, 8336–8342. [[CrossRef](#)]
37. Zhang, Q.; Li, C.; Li, T. UV/H₂O₂ Process Under High Intensity UV Irradiation: A Rapid and Effective Method for Methylene Blue Decolorization. *CLEAN Soil Air Water* **2013**, *41*, 1201–1207. [[CrossRef](#)]
38. Hisaindee, S.; Meetani, M.A.; Rauf, M.A. Application of LC-MS to the analysis of advanced oxidation process (AOP) degradation of dye products and reaction mechanisms. *TrAC Trends Anal. Chem.* **2013**, *49*, 31–44. [[CrossRef](#)]
39. He, Y.; Grieser, F.; Ashokkumar, M. The mechanism of sonophotocatalytic degradation of methyl orange and its products in aqueous solutions. *Ultrason. Sonochem.* **2011**, *18*, 974–980. [[CrossRef](#)] [[PubMed](#)]

40. Meetani, M.A.; Hisaindee, S.M.; Abdullah, F.; Ashraf, S.S.; Rauf, M.A. Liquid chromatography tandem mass spectrometry analysis of photodegradation of a diazo compound: A mechanistic study. *Chemosphere* **2010**, *80*, 422–427. [[CrossRef](#)] [[PubMed](#)]
41. Siegbahn, P.E.M.; Blomberg, M.R.A. Mechanisms for enzymatic reactions involving formation or cleavage of O-O bonds. *Theor. Comput. Chem.* **2001**, *9*, 95–143. [[CrossRef](#)]
42. Zhang, X.; Li, X.; Jiang, Y.; Hu, M.; Li, S.; Zhai, Q. Combination of enzymatic degradation by chloroperoxidase with activated sludge treatment to remove sulfamethoxazole: Performance, and eco-toxicity assessment. *J. Chem. Technol. Biotechnol.* **2016**, *91*, 2802–2809. [[CrossRef](#)]
43. Hager, L.P.; Morris, D.R.; Brown, F.S.; Eberwein, H. Chloroperoxidase II. Utilization of Halogen Anions. *J. Biol. Chem.* **1966**, *241*, 1769–1777. [[PubMed](#)]
44. Correia, V.M.; Stephenson, T.; Judd, S.J. Characterisation of textile wastewaters—A review. *Environ. Technol.* **1994**, *15*, 917–929. [[CrossRef](#)]
45. Silva, M.C.; Corrêa, A.D.; Amorim, M.T.S.P.; Parpot, P.; Torres, J.A.; Chagas, P.M.B. Decolorization of the phthalocyanine dye reactive blue 21 by turnip peroxidase and assessment of its oxidation products. *J. Mol. Catal. B Enzym.* **2012**, *77*, 9–14. [[CrossRef](#)]
46. *Ecological Effects Test Guidelines OCSPP 850.4100: Seedling Emergence and Seedling Growth*; United States Environmental Protection Agency, National Service Center for Environmental Publications (NSCEP): Cincinnati, OH, USA, 2012.



© 2017 by the authors. Licensee MDPI, Basel, Switzerland. This article is an open access article distributed under the terms and conditions of the Creative Commons Attribution (CC BY) license (<http://creativecommons.org/licenses/by/4.0/>).